

Letters to the Editor

Interaction of nanodiamond with in situ generated sp-carbon chains probed by Raman spectroscopy

Ladislav Kavan^{a,*}, Marketa Zukalova^a, Martin Kalbac^a, Eiji Ōsawa^b, Lothar Dunsch^c

^a J. Heyrovský Institute of Physical Chemistry, Academy of Sciences of the Czech Republic, Dolejškova 3, 18223 Prague 8, Czech Republic

^b NanoCarbon Research Institute Ltd., Rm. 301, Toudai Kashiwa Ventura Plaza, 5-4-19 Kashiwa-no-ha, Kashiwa, Chiba 277-0882, Japan

^c Leibniz Institute of Solid State and Materials Research, Helmholtzstr. 20, D-01069 Dresden, Germany

Received 7 July 2006; accepted 11 August 2006

Available online 12 September 2006

Keywords: Carbyne; Diamond; Raman spectroscopy

A carbon allotrope containing solely linear sp-carbon chains (carbyne) [1] has not yet been demonstrated convincingly, but composite carbonaceous structures containing sp/sp² carbon atoms attract increasing attention. Among various challenges, the possible occurrence of sp-carbon chain in the interior of carbon nanotube [2] and its formation during heat treatment of double wall carbon nanotubes [3] have been discussed recently.

In 1994, Heimann [4] suggested that sp-carbon chains may play a role as intermediates during shock-induced transformation of graphite into diamond. Indeed, diamond was found in the products of shock compression of carbynoid material grown by dehydrohalogenation of poly(vinylidene halide) [1,5]. An opposite effect, i.e., formation of carbyne via shock-compression of diamond was observed, too [6]. Interestingly, carbyne was found in a diamond mine in China [7], but geochemical aspects of the carbyne/diamond conversion are unknown.

Sun et al. [8] prepared diamond by pyrolysis (600 °C) of poly(phenylcarbyne), (PhC)_n made by total dechlorination of α,α,α-trichlorotoluene [9]. This reaction is an explicit demonstration of terminological inconsistency of carbyne: the (PhC)_n is solely sp³-bonded polymer, in which the name “carbyne” is correctly used in terms of the IUPAC-codified name for a triply bonded carbon radical. Curiously, various sp-bonded carbon allotropes (also termed “carbyne” in historical sense) were found in the products of pyrolysis

(1000–1600 °C) of poly(phenylcarbyne), (PhC)_n along with cubic and hexagonal diamond [9].

Kudryavtsev and Evsyukov [10] reported on diamond growth in dehydrohalogenated poly(vinylidene chloride) mixed with a catalytic amount (1 wt.%) of ultra-dispersed diamond. The growth took place at 360–370 °C and atmospheric pressure, but the mechanism for catalytic diamond growth remained unknown. Here we report on a variant of this synthesis, in which the sp-chains were generated in situ from a mixture of poly(tetrafluoroethylene) PTFE with nanodiamond (nD) by the action of gaseous potassium. This study has been motivated by the fact that the ex-PTFE sp-chains are of exceptional quality [1,11] compared to other chemically synthesized analogues, and, secondly, the reaction can be carried out with a complete exclusion of air oxygen and humidity. As the sp-carbon chains are extremely reactive, the absence of any undesired reactant is a prerequisite for detailed studies of their reactions and structural modifications. Also the nanodiamond used by Kudryavtsev and Evsyukov [10] has been revealed to be composed of submicron-sized aggregates of primary particles [12]. Hence, it would be challenging to use the primary particles of nD with 4–5 nm in diameter [13] instead of their aggregates.

The sample of primary nD particles used in this work was prepared by disintegrating of the commercial ultradispersed diamond, which in turn was isolated as grey powder by oxidizing detonation soot from TNT–RDX explosion with hot nitric acid, washing with water and drying at 120 °C for 12 h [14]. Disintegration of aggregates was

* Corresponding author. Fax: +420 2 8658 2307.

E-mail address: kavan@jh-inst.cas.cz (L. Kavan).

accomplished by beads milling with an Apex Mill from Kotobuki Ind. Co. using 30 μm zirconia beads stabilized with yttrium. Conditions of beads-milling are described in detail elsewhere [15,16]. After final sonication and centrifugal separation of uncrushed larger particles, the resulting colloidal solution contained about 10 wt.% of dispersed primary particles of cubic nD with diamond purity of 93% as determined by quantitative X-ray diffraction intensity analysis using ZnO as internal standard.

The above described aqueous suspension of nD was evaporated to dryness at room temperature and re-dispersed in absolute ethanol under sonication. Poly(tetrafluoroethylene) (PTFE) powder from Aldrich was treated in absolute ethanol under sonication and then mixed with the ethanolic suspension of nanodiamond in concentrations of 10 wt.% or 20 wt.% of nD in PTFE. The mixture was sonicated at ca. 40 °C while part of ethanol evaporated and the mixture attained a consistence of viscous slurry. The slurry was visually homogeneous, and no phase separation was observed during its storage at room temperature. The slurry was finally evaporated on a glass support, leaving a reasonably compact and homogeneous film of ca. 1 cm^2 in area. On the same glass support, two other pieces of films were deposited, viz., films from pure nD, and from pure PTFE, respectively. They were deposited, in the same way, by evaporating of the corresponding ethanolic slurries.

The glass supported films of nD, PTFE and nD/PTFE mixtures were outgassed at 300 °C in vacuum (10^{-5} Pa) and sealed in a cell with glass optical window. Potassium metal (from BDH) was purified by repeated distillation in vacuum, and finally transferred into the reaction cell via a breakable glass joint. The all-glass reaction cell was finally sealed in high vacuum, while the sample layers were not in contact to solid potassium. The reaction of potassium vapor with the PTFE and nD/PTFE was initiated by increasing the temperature. The reaction of potassium vapor manifested itself by blackening of PTFE already after several minutes at 100 °C.

The Raman spectra were excited by Ar^+ laser (Innova 300 series, Coherent) and recorded by a T-64000 spectrometer (Instruments, SA) interfaced to an Olympus BH2 microscope. The laser power impinging on the cell window was between 2 and 3 mW. The Raman spectra were measured via the glass optical window (without opening the cell) by the 50 \times objective of large focus distance. The Raman spectrometer was calibrated before each set of measurements by using for reference the F_{1g} line of Si at 520.2 cm^{-1} . All frequencies and intensities were normalized against those of the Si-line.

Fig. 1 shows the results of Raman monitoring of gradual conversion of PTFE into carbonaceous products. It is obvious that the disappearance of the Raman features of PTFE is accompanied by the rise of new bands around 2000 cm^{-1} , which are characteristic for sp-carbon chains [1,17]. At early stages of the reaction, we note double peak features at ca. 1910 cm^{-1} and 2050 cm^{-1} ('2' in Fig. 1). This

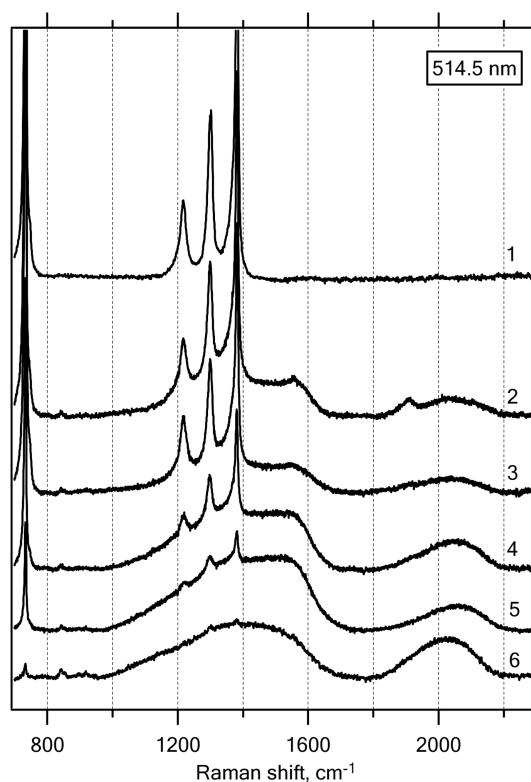


Fig. 1. Raman spectra at 514.5 nm excitation. From top to bottom: (1) pure PTFE, (2) *ditto* reacted with K-vapor at 100 °C for 15 min, (3) 100 °C for 1 h, (4) 100 °C for 2 h, (5) 100 °C for 12 h, (6) 150 °C for 12 h. The reactions were sequential, i.e., the product of an earlier treatment served as precursor of the next treatment. Spectra are offset for clarity, but their intensity scales are identical.

structure disappears as the reaction progresses ('3' in Fig. 1), being replaced by a single broad peak at 2050 cm^{-1} , which shifts to lower wave numbers at later stages of the reaction ('4'–'6' in Fig. 1). This spectral development is compatible with the hypothesis that PTFE converts first into short oligocumulenic segments, and finally into polyynes [1,17]. Whereas the conversion of PTFE into polyynes is well documented in the previous literature [1,17], here we show for the first time these intermediate moieties at the early stages of the PTFE defluorination.

The Raman spectra of the nD/PTFE composite are shown in Fig. 2 (curves A, B). Obviously, they exhibit features of superposition of the Raman spectra of the individual components, viz., pure PTFE (curve 1, Fig. 1) and pure nD (curve C, Fig. 2). The spectral superposition even reflects the effect of strong photoluminescence background of nanodiamond, which is more pronounced for the composite containing larger amount of nD (cf. curves A, B in Fig. 2). After defluorination with K-vapor, the photoluminescence background disappears completely (cf. curves D, E in Fig. 2). The nanodiamond peak at 1630 cm^{-1} disappears after the defluorination of PTFE, while the peak at 1324 cm^{-1} is still clearly visible. We can obviously exclude that this feature is a remnant of the peaks of PTFE, since

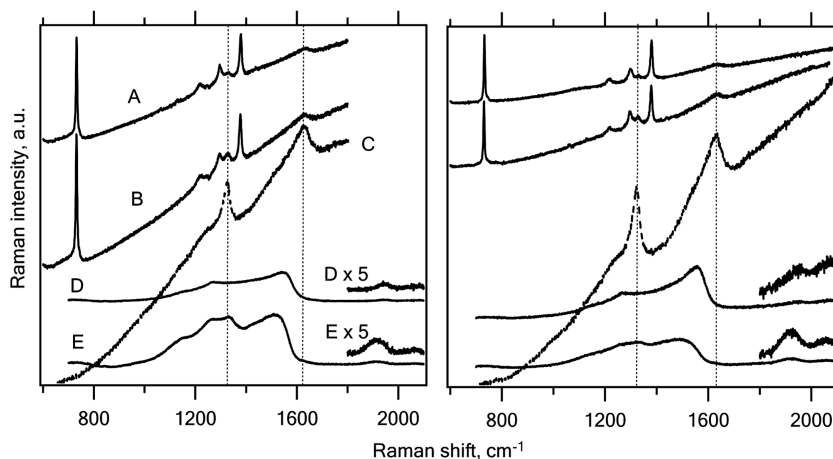


Fig. 2. Raman spectra at 514.5 nm excitation (left chart) and 488 nm excitation (right chart). (A) nD/PTFE; 10 wt.% nD, (B) nD/PTFE; 20 wt.% nD, (C) pure nD, (D) nD/PTFE (10 wt.% nD) after reaction with K-vapor at 150 °C for 12 h, (E) nD/PTFE (20 wt.% nD) after reaction with K-vapor at 150 °C for 12 h. Details of spectra D and E after 5× zooming are also shown. Spectra are offset for clarity, but their intensity scales are identical. Dashed lines label the frequencies, at which the characteristic features of nD occur.

the strong diagnostic peak of PTFE at 732 cm^{-1} is missing in the spectra represented by curves D, E (Fig. 2). This confirms that the defluorination of PTFE was complete. The Raman spectra of both nanodiamond and sp-carbon chains are resonantly enhanced, and the enhancement for sp-carbon is more pronounced at the 488 nm laser excitation [17].

The sp-carbon chains, which are produced by K-vapor treatment of PTFE (cf. Fig. 1) are almost completely quenched by the presence of nanodiamond (curves D, E on Fig. 2). We only trace weak features, similar to those in incompletely defluorinated PTFE at early stages of the reaction with K-vapor (Fig. 1, curve 2). Also the sp^2 carbon features in defluorinated PTFE and nD/PTFE composite are significantly different. In the second case, we can trace better developed D- and G-features typical for polycrystalline graphite. These results are compatible with a hypothesis that the in situ produced sp-carbon chains from PTFE readily react with the nanodiamond. The nanodiamond seems to promote the conversion of sp to sp^2 carbon, but the conversion of sp to sp^3 is less supported by our Raman data. We did not find Raman signal of larger diamond crystals, even in the material, which was removed from the vacuum cell and washed with water in contact to air. A typical Raman spectrum of this end product was similar to that of the starting nD material (cf. curve C in Fig. 2). Hence, we suggest that the nanodiamond acts as a catalyst for the sp/ sp^2 conversion. Our Raman analysis did neither reveal any sign of sp-hybridized carbon crystals (“carbyne”), nor any visible growth of diamond.

Acknowledgements

This work was supported by IFW-Dresden, by the Academy of Sciences of the Czech Republic (Contract No. A4040306), by the Czech Ministry of Education,

Youth and Sports (Contract No. LC-510) and by NEDO International Grant (Contract. No. 20041T081).

References

- [1] Heimann RB, Evsyukov SE, Kavan L. Carbyne and carbynoid structures, physics and chemistry of materials with low-dimensional structures, vol. 21. Dordrecht: Kluwer Academic Publishers; 1999.
- [2] Jinno M, Ando Y, Bandow S, Fan J, Yudasaka M, Iijima S. Raman scattering study of heat treated carbon nanotubes. *Chem Phys Lett* 2006;418:109–14.
- [3] Fantini C, Cruz E, Jorio A, Terrones M, Terrones H, Van Lier G, et al. Resonance Raman study of linear carbon chains. *Phys Rev B* 2006;73:193408–1934084.
- [4] Heimann RB. Linear finite carbon chains (carbyne): Their role during dynamic transformation of graphite to diamond, and their geometric and electronic structure. *Diamond Relat Mater* 1994;3: 1151–7.
- [5] Komatsu T, Nomura M, Kakudate Y, Fujiwara S, Heimann RB. Characterization of dehydrochlorinated poly(vinylidene chloride) and the shock-compressed material. *Macromol Chem Phys* 1995;196: 3031–40.
- [6] Yamada K, Burkhard G, Dan K, Tanabe Y, Sawaoka AB. Microstructures of carbon polymorphs formed in shocked compressed diamond powder utilizing an interaction of oblique shock waves. *Carbon* 1994;32:1197–213.
- [7] Chuan XY, Zheng Z, Chen J. Flakes of natural carbyne in a diamond mine. *Carbon* 2003;41:1877–80.
- [8] Sun Z, Sun Y, Wilson SR. Diamond-like carbon from carbyne. *Thin Solid Films* 2000;377–378:203–7.
- [9] Visscher GT, Nesting DC, Badding JV, Bianconi PA. Poly(phenylcarbyne): A polymer precursor to diamond-like carbon. *Science* 1993;260:1496–9.
- [10] Kudryavtsev YP, Evsyukov SE. Formation of diamond from carbyne. *Diamond Relat Mater* 1997;6:1743–6.
- [11] Liang TT, Yamada Y, Yoshizawa N, Shiraishi S, Oya A. Preparation of porous carbon by defluorination of PTFE. *Chem Mater* 2001;13:2933–9.
- [12] Kruger F, Kataoka F, Ozawa M, Fujino T, Suzuki Y, Aleksenskii AE, et al. Unusually tight aggregation in detonation nanodiamond: Identification and disintegration. *Carbon* 2005;43:1722–30.
- [13] Aleksenskii AE, Baidakova MV, Vul AY, Siklitskii VI. The structure of diamond nanoclusters. *Phys Solid State* 2006;41: 668–71.

- [14] Shenderova OA, Zhirnov VV, Brenner DW. Carbon nanostructures. *CRC Crit Rev Solid State Mater Sci* 2002;27:227–356.
- [15] Panich AM, Shames AI, Vieth HM, Osawa E, Vul AY. Nuclear magnetic resonance study of ultrananocrystalline diamonds. *Eur J Phys*, in press.
- [16] Ozawa M, Inakuma M, Takahashi M, Kataoka F, Kruger F, Osawa E. Preparation and behavior of brownish clear nanodiamond colloids. *Adv Mater*, in press.
- [17] Kastner J, Kuzmany H, Kavan L, Dousek FP, Kürti J. Electrochemical preparation of carbyne with high yield. An in situ Raman scattering study. *Macromolecules* 1995;28:344–53.

Controlling water contact angle on carbon surfaces from 5° to 167°

Aihui Yan, Xingcheng Xiao, Indrek Külaots, Brian W. Sheldon, Robert H. Hurt *

Brown University, Division of Engineering, 182 Hope Street, Providence, RI 02912, United States

Received 7 July 2006; accepted 6 August 2006

Available online 7 September 2006

Keywords: Surface properties; Surface treatment; Carbon films

The interaction of liquid water with graphenic carbon surfaces is important for nanotube dispersion and processing [1], nanotube fluidics [2,3], aqueous phase sorbent applications [4], protein adsorption and cell behaviour on carbon implant surfaces [5], and the rates of cell uptake and biological membrane translocation that influence nanomaterial toxicity [6]. In many carbon applications one wishes to decrease contact angle to improve aqueous dispersion [1] or increase biocompatibility [5], but there is also interest in systematically *increasing* contact angle, in particular into the so-called superhydrophobic range beyond 150° to create water-repelling, surface-cleaning surfaces [7]. The technique used most often to increase hydrophilicity (decrease water contact angle) is surface oxidation, where there are a range of competing oxidants and treatment protocols, but very few studies comparing quantitative water contact angles. Recently Mattia et al. [2,8] report enhanced hydrophilicity upon NaOH treatment using CVD films as models for nanotubes and nanopipes. Several recent studies in the nanotube literature use aryl-sulfonation through diazonium salt chemistry to improve nanotube dispersion [1]. This treatment may extend the range of carbon hydrophilicity, but quantitative comparisons of this and other treatments based on contact angle have not been made to our knowledge.

Much of the recent work on carbon surface chemistry is targeted at nanomaterials, which are difficult and inconvenient subjects for quantitative hydrophilicity characteriza-

tion. Here we adopt carbon films as model systems for the study of surface chemistry and apply the simple sessile drop technique to compare a variety of chemical surface treatments.

In this study, we fabricate carbon films on quartz slides by physical vapour deposition (PVD), liquid-crystal (LC) spin coating and then carbonization [9], and microwave plasma-enhanced chemical vapor deposition (PECVD); and treat them with a variety of reagents including HNO₃, O₃, NaOH, and sulfanilic acid with sodium nitrite. Most of the experiments are performed on LC-derived films, which are smooth (as-prepared 2.6 nm RMS roughness by AFM) and reveal the effects of surface chemistry independent of the complex effects of roughness. Fig. 1 shows example images of our sessile drops on the various films showing the full range of wetting behavior from 5° to 167° for the equilibrium contact angle. The wetting experiments were done at room temperature in air and quantitative contact angles reported as averages of 2–7 droplets (each 1–5 μL) with the standard error of the mean reported in Table 1.

Table 1 and Fig. 2 summarize the data from this study. The cleaved HOPG (SPI-1 Grade) basal surface and the polyaromatic edge plane of quenched mesophase pitch are similarly hydrophobic with water contact angles near 90°. This suggests that graphene/polyaromatic plane orientation is not a significant factor in carbons if the edge-planes are fully hydrogenated. It further suggests that the low contact angles and large variations in angle seen (5–90° in the smooth films) are primarily due to non-hydrogenated defect sites and heteroatom (O,N,S) functionalization.

* Corresponding author. Tel. +1 4018632685; fax: +1 4018639120.
E-mail address: Robert_Hurt@brown.edu (R.H. Hurt).